

# Unified Description of Aging and Rate Effects in Yield of Glassy Solids

Jörg Rottler<sup>1</sup> and Mark O. Robbins<sup>2</sup>

<sup>1</sup>*Princeton Institute for the Science and Technology of Materials (PRISM), Princeton University, Princeton, New Jersey 08544, USA*

<sup>2</sup>*Department of Physics and Astronomy, Johns Hopkins University, 3400 North Charles Street, Baltimore, Maryland 21218, USA*

(Received 22 June 2005; published 22 November 2005)

The competing effects of slow structural relaxations (aging) and deformation at constant strain rate on the shear yield stress  $\tau^y$  of simple model glasses are examined using molecular simulations. At long times, aging leads to a logarithmic increase in density and  $\tau^y$ . The yield stress also rises logarithmically with rate but shows a sharp transition in slope at a rate that decreases with increasing age. We present a simple phenomenological model that includes both intrinsic rate dependence and the change in properties with the total age of the system at yield. As predicted by the model, all data for each temperature collapse onto a universal curve.

DOI: [10.1103/PhysRevLett.95.225504](https://doi.org/10.1103/PhysRevLett.95.225504)

PACS numbers: 81.05.Kf, 61.43.Fs, 62.20.Fe, 83.60.La

The mechanical behavior of amorphous materials such as polymers [1] and bulk metallic glasses [2] continues to present great theoretical challenges. While dislocations have long been recognized as playing a central role in plasticity of crystalline systems, no counterpart is easily identifiable in disordered matter. In addition, yield and flow [3] occur very far from equilibrium, where the state of the system may have a complex history dependence.

Progress towards understanding yield in glassy systems is currently being made through a combination of simple models and particle-based simulations. Falk and Langer's rate-equation-based shear transformation zone (STZ) theory [4] was inspired by simulations, and extensions of the theory [5,6] have been able to reproduce many aspects of experiments. A valuable alternative approach is based on the energy landscape picture of glasses, which relates well to the zero temperature, zero strain rate limit of plasticity [7,8]. Yet another intriguing approach uses discretizations of continuum elasticity theory to describe the long-range interactions of shear yielding regions and resulting localization phenomena (shear bands) [9]. A truly "*ab initio*," but very challenging, approach to strained glasses is presently being pursued by extending the mode-coupling theory of the glass transition to the effects of an external drive [10–12].

Recent molecular simulations of simple model glasses have revealed that shear occurs through local deformations [4] whose quadrupolar strain energy fields are consistent with STZs [8]. The mean yield stress  $\tau^y$  satisfies a generalized von Mises shear yield criterion under general loading conditions as long as failure is homogeneous [13]. However, results for the rate and temperature dependence of  $\tau^y$  [14] are inconsistent with the simple, but widely used, Eyring model of viscoplasticity. These results and the statistics of local yield events [8,14] suggest that, in shearing glasses, quantities other than the thermodynamic temperature contribute to the activation of plastic events, although the precise nature of this "effective temperature" [15] remains uncertain.

In addition to the above control parameters, experiments show that the yield stress is sensitive to the age of the glass [16]. Since glasses are out-of-equilibrium structures, they exhibit a slow, but never ceasing, intrinsic aging dynamics [17,18]. In a simple picture, aging can be thought of as thermally activated hopping in the glassy energy landscape [17]. With longer aging time, the system is able to pack more densely and reach deeper and deeper energy minima. As a result, the stress required to bring the system out of the local minimum into a flowing configuration increases with waiting time [19]. This scenario is reflected in the soft glassy rheology model, which predicts a slow logarithmic increase of the yield stress with increasing aging time [20].

Our previous studies of shear yielding used a molecular glass that was prepared through a rapid quench from the liquid state [14]. The aging or waiting time  $t_w$  in the glassy regime before the application of stress was typically shorter than the time to reach the yield point, a situation not particularly common in experiments. The computational effort to reach substantially longer waiting times used to be prohibitive, but improvements in computing power are now making it possible to study the relationship between aging and shear yielding in molecular glasses. A first study of this kind was presented by Varnik *et al.* [21], who showed for one fixed glassy temperature and one fixed strain rate that the yield stress increases with age. In the present work, we undertake a more systematic study of shear yielding in the rate-age-temperature parameter space and develop a phenomenological model that describes the complex effects of all these parameters on the shear strength of the glassy solid.

The methodology in the present work builds on previous studies [13,14] and uses the 80:20 binary Lennard Jones (LJ) mixture [22] that has been employed extensively in molecular dynamics studies of glasses. Our units are the binding energy  $u_0$  and length  $a$  of the LJ potential between majority particles. The characteristic time is  $t_{LJ} = (ma^2/u_0)^{1/2}$ , where  $m$  is the mass of the particles. When all interactions are truncated at particle separations greater

than  $r_c = 1.5a$ , the model exhibits a glass transition at a temperature  $T_g \approx 0.3u_0/k_B$  [14].

We begin by preparing a melt configuration composed of 32 768 particles at  $T = 1.3u_0/k_B$  and then quench rapidly at constant volume to a glassy temperature  $T = 0.2u_0/k_B$  over a time of  $750t_{LJ}$ . The initial density is chosen so that the hydrostatic pressure  $p$  is close to zero at this temperature. We then quench to the desired temperature and wait a time  $t_w$ , while maintaining zero pressure. The density increases with waiting time in a logarithmic fashion, in agreement with the intuitive idea that aging allows the material to optimize its local packing [16]. A 0.6% change is observed from  $t_w = 750$  to  $750\,000t_{LJ}$  at  $T = 0.2u_0/k_B$ . As expected for an unstrained system, the rate of relaxation decreases with decreasing thermodynamic temperature, becoming too small to detect at  $T = 0.01u_0/k_B$ .

After aging, a volume conserving shear is applied to the initially cubic simulation cell. The strain along the  $z$  direction,  $\epsilon_{zz}$ , increases at a constant rate  $\dot{\epsilon}$ , and the strains along the two perpendicular directions are decreased symmetrically to maintain fixed volume. As in previous work [13], we identify the shear yield stress  $\tau^y$  with the maximum of the deviatoric stress  $\tau \equiv [(\sigma_1 - \sigma_2)^2 + (\sigma_2 - \sigma_3)^2 + (\sigma_3 - \sigma_1)^2]^{1/2}/3$ , where the  $\sigma_i$  are the principal stresses. The strain at yield,  $\epsilon^y$ , is typically between 5% and 10% for all cases studied.

Figure 1(a) shows  $\tau^y$  as a function of waiting time for four different strain rates from  $\dot{\epsilon} = 10^{-6}$  to  $10^{-3}t_{LJ}^{-1}$  at  $T = 0.2u_0/k_B$ . For all rates, the yield stress increases logarithmically at long waiting times, and the slope  $s_0$  is independent of rate. Note that the changes in  $\tau^y$  are too large to be explained by the increase in density with age discussed above. Thus, the local internal structure in the glass must also evolve logarithmically in time. At short times and low shear rates, our results deviate from the logarithm, becoming nearly independent of  $t_w$ . This crossover is explained below [Eq. (2)].

As shown in Fig. 1(b), a logarithmic dependence on waiting time is also observed at lower temperatures. Data for a relatively high rate ( $10^{-4}t_{LJ}^{-1}$ ) is shown in order to avoid the plateau seen at low  $t_w$  and  $\dot{\epsilon}$  in Fig. 1(a). The simplest picture of thermal activation in an energy landscape would suggest that the slope  $s_0$  scales linearly with temperature. The inset in Fig. 1(b) shows that our data are generally consistent with  $s_0 \propto T$ . The value for  $T = 0.01u_0/k_B$  lies above the linear fit, but the change in  $\tau^y$  is very small at this temperature and the data may be dominated by an initial transient.

We now turn to the combined effect of strain rate and aging on the yield stress. Figure 2 examines  $\tau^y$  as a function of strain rate over 3 orders of magnitude in waiting time at  $T = 0.2u_0/k_B$ . The data obtained with the shortest time,  $t_w = 750t_{LJ}$  (lowest curve), increase slowly with rate at low rates and more rapidly at higher rates. This waiting time corresponds to the one used in our earlier

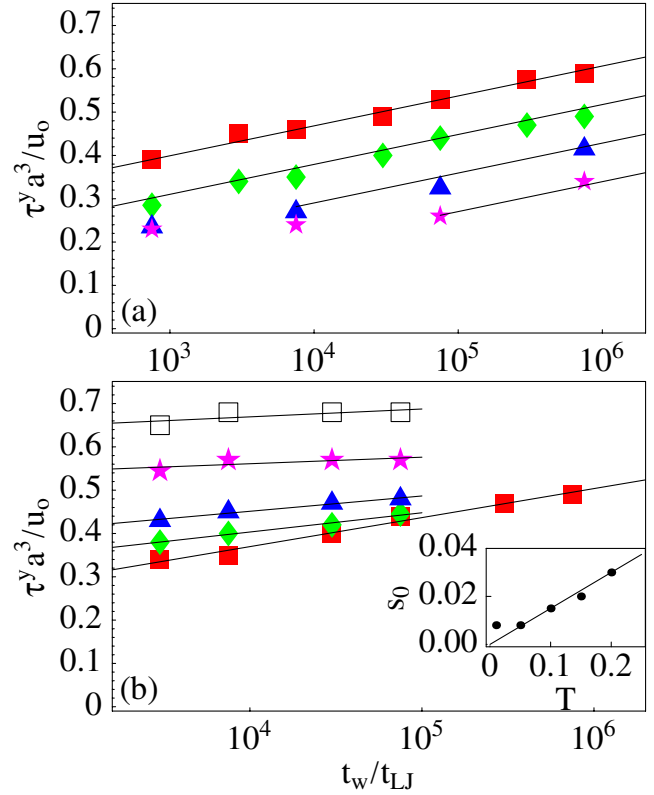


FIG. 1 (color online). Shear yield stress as a function of waiting time. (a) Four different rates  $\dot{\epsilon} = 10^{-3}t_{LJ}^{-1}$  (■),  $10^{-4}t_{LJ}^{-1}$  (◆),  $10^{-5}t_{LJ}^{-1}$  (▲), and  $10^{-6}t_{LJ}^{-1}$  (☆) at  $T = 0.2u_0/k_B$ . The solid line fits to the large  $t_w$  region have common slope  $s_0$ , and successive lines are separated by the vertical shift  $s_1 \ln(10)$  predicted by Eq. (2). (b) Five different temperatures  $T = 0.2u_0/k_B$  (■),  $0.15u_0/k_B$  (◆),  $0.1u_0/k_B$  (▲),  $0.05u_0/k_B$  (☆), and  $0.01u_0/k_B$  (□) at fixed rate  $\dot{\epsilon} = 10^{-4}t_{LJ}^{-1}$ . The solid lines are logarithmic fits to the data at each  $T$ , and their slopes  $s_0$  are plotted against  $T$  in the inset. The straight line in the inset is a linear fit through the origin.

study of rate dependence [14]. There we showed that the small rate part of the curve could be fitted to a logarithmic rate dependence with very little change in the prefactor  $s'$  of the logarithm with  $T$ . Here we see that the region of rapid rate dependence moves to lower rates as  $t_w$  increases. For the longest  $t_w$ , the entire curve can be fit by a logarithmic rate dependence with a higher slope  $s_1 = 0.037$ . We will refer to the regimes of low and steep slope as regimes I and II, respectively. Note that there may also be a third regime at still higher rates where the strain is faster than local elastic relaxations of the solid. As discussed in Ref. [14], this may be reached when  $\dot{\epsilon}c/L \sim 1$ , where  $c$  is the speed of sound in the glass and  $L$  the scale of elastic heterogeneity. However, this regime is unlikely to be accessible to experiments.

Varnik *et al.* also observed a crossover between regimes I and II that moved to lower rates with increasing waiting time [21]. They argued that the crossover is asso-

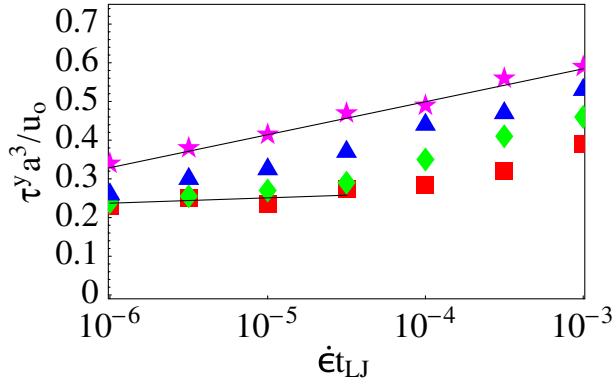


FIG. 2 (color online). Shear yield stress as a function of rate for 4 different waiting times  $t_w = 750 t_{LJ}$  (■),  $7500 t_{LJ}$  (◆),  $75000 t_{LJ}$  (▲), and  $750000 t_{LJ}$  (☆) at  $T = 0.2 u_0 / k_B$ . The solid lines indicate logarithmic fits with slopes of  $s_1 = 0.037$  and  $s' = 0.006$  for long and short waiting times, respectively. Error bars are comparable to the symbol size.

ciated with shearing the system faster than its structural relaxation time, noting evidence [18] that the time  $t_{\text{cage}}$  for atoms to escape from local cages is comparable to  $t_w$ . However, a data collapse motivated by this picture did not describe their data. Moreover, we have evaluated  $t_{\text{cage}}$  from diffusion and the decay of the incoherent scattering function [18] and find  $t_{\text{cage}}$  increases much more rapidly than  $t_w$ , particularly at lower temperatures. As we now show, a different physical picture based only on the total effective age of the system can resolve these discrepancies and explain a wide range of numerical data.

A logarithmic dependence on both waiting time and rate is commonly observed in friction experiments [23,24]. In this context, phenomenological “rate-state” models have captured many experimental results. Such models assume that the response of the system depends on both the rate of sliding and on a single “state variable”  $\theta$  that corresponds to the effective age of the system. Replacing the friction force and sliding velocity in these models by the yield stress and strain rate yields

$$\tau^y = \tau_0 + s_0 \ln(\theta / t_{LJ}) + s_1 \ln(\dot{\epsilon} t_{LJ}), \quad (1)$$

where the first logarithm reflects the growth in yield stress with increasing age that is typical of thermally activated systems, and the second is the increase in  $\tau^y$  with shear rate for a fixed state of the system. An evolution equation for  $\theta$  must be specified to complete the model. We write  $\dot{\theta} = f(\epsilon_{zz}, T)$  to allow for changes in the rate of aging and rejuvenation during strain. Choosing the normalization  $f(0, T) = 1$  guarantees that  $\theta$  equals the age  $t_w$  at the end of the waiting interval, and integrating to find  $\theta$  at the yield strain  $\epsilon_y$  gives:

$$\tau^y = \tau_0 + s_0 \ln(t_w / t_{LJ} + \alpha / \dot{\epsilon} t_{LJ}) + s_1 \ln(\dot{\epsilon} t_{LJ}), \quad (2)$$

where  $\alpha \equiv \int_0^{\epsilon_y} d\epsilon_{zz} f(\epsilon_{zz}, T)$ . If  $f$  is assumed to be independent of strain,  $\alpha = \epsilon^y$ , and  $\alpha / \dot{\epsilon}$  just corresponds to the time  $t^y$  to strain the system to yield. If rejuvenation begins

before  $\epsilon^y$ ,  $\alpha$  will be smaller. Strain may also accelerate aging [25] by lowering energy barriers, leading to larger values of  $\alpha$ .

Equation (2) captures all of the limiting behavior seen in our numerical results. For fixed shear rate, only the first logarithm is relevant. At long waiting times,  $\tau^y$  increases as  $s_0 \ln(t_w)$  with a rate independent slope  $s_0$  and an offset that rises as  $s_1 \ln(\dot{\epsilon} t_{LJ})$ . This behavior is observed in Fig. 1(a) at long  $t_w$ . The saturation of  $\tau^y$  at small  $t_w$  arises because, for  $t_w < \alpha / \dot{\epsilon}$ , the state of the system is dominated by aging during the straining interval. For fixed waiting time, Eq. (2) contains the two regimes observed in Fig. 2. When  $t_w$  is smaller than  $\alpha / \dot{\epsilon}$  (regime I),  $t_w$  is irrelevant and the two logarithms compete. A higher rate increases the intrinsic strength through the second logarithm in Eq. (2) but allows less time for aging to increase the yield stress through the first logarithm. The net result is that  $\tau^y$  rises as  $s' \ln(\dot{\epsilon})$ , where  $s' = s_1 - s_0$  is smaller than either  $s_1$  or  $s_0$ . For large  $t_w$  (regime II), only the second logarithm in Eq. (2) contributes and  $\tau^y$  rises as  $s_1 \ln(\dot{\epsilon})$ . Here the solid is strained so rapidly that it does not age significantly before yield occurs.

Equation (2) also implies that data for all waiting times and shear rates should collapse onto a universal curve if  $\tau^y + s' \ln(t_w / t_w^0)$  is plotted against  $\dot{\epsilon} t_w$ , where  $t_w^0$  is any reference time. Figure 3 shows the success of this collapse over the whole temperature range. There are no adjustable parameters in the collapse, since  $s' = s_1 - s_0$  was determined from separate measurements of  $s_1$  and  $s_0$  in the asymptotic regimes of plots like Figs. 1 and 2.

The solid lines in Fig. 3 show the predictions of Eq. (2). These lines do require fits to  $\tau_0$  and  $\alpha$  for each  $T$ . The crossover between regimes I and II occurs when  $\dot{\epsilon} t_w \approx \alpha$ , and  $\alpha$  clearly increases by more than an order of magnitude with decreasing temperature. For  $T = 0.2 u_0 / k_B$ , the best fit gave  $\alpha = 0.02$  with an uncertainty of about a factor of 2 due to the error bars on  $s_0$  and  $s_1$ . Note that this range of  $\alpha$  is comparable to  $\epsilon^y$ , implying that the rate of aging during strain is comparable to that at zero strain. The increase in  $\alpha$  with decreasing  $T$  implies that the aging is accelerated by strain at low temperatures. Our previous studies of the rate

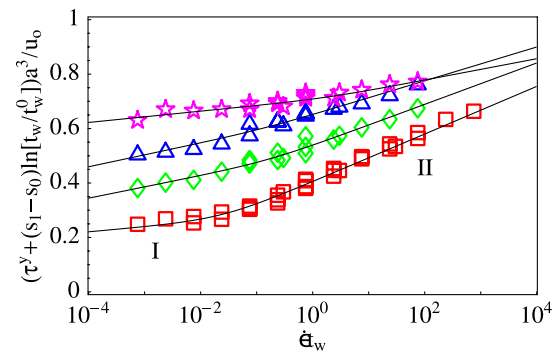


FIG. 3 (color online). Plot of data for all  $t_w$  and  $\dot{\epsilon}$  at  $T = 0.2 u_0 / k_B$  (□),  $0.1 u_0 / k_B$  (◇),  $0.05 u_0 / k_B$  (△), and  $0.01 u_0 / k_B$  (☆) and universal curves (solid lines) predicted by Eq. (2).

of structural rearrangements in strained and unstrained glasses [14] support these conclusions. The probability distribution of sudden local stress and strain changes was monitored as a function of the applied strain at different  $T$ . Very near  $T_g$ , the rate and magnitude of local changes is nearly independent of the applied strain, explaining why  $\alpha \approx \epsilon^y$ . At low  $T$ , the probability of large events increases rapidly with strain, becoming comparable to the rate at  $T_g$  near the yield point. In this regime, most of the thermal activation occurs at strains near the yield point leading to  $\alpha \gg \epsilon^y$ .

Equation (2) can also be obtained from a simple modification of Eyring's model [26] of stress-assisted thermal activation over energy barriers of height  $\Delta E$ . In this very simple but commonly used model, the strain rate is associated with transition rates over barriers whose height decreases linearly with applied stress. One obtains  $\tau^y = \Delta E/V^* + (k_B T/V^*) \ln[\dot{\epsilon}/\nu_0]$ , where  $V^*$  is a constant called the "activation volume" and  $\nu_0$  an attempt frequency. This model provides a basic explanation for logarithmic rate behavior but does not include aging. A suitable, albeit *ad hoc*, extension is to include an increase in  $\Delta E$  with the total age of the system, as, for instance,  $\Delta E = \Delta E_0 + f(T) \ln[(t_w + \alpha/\dot{\epsilon})/t_{LJ}]$ . This immediately yields Eq. (2) with  $\tau_0 = \Delta E/V^*$ ,  $s_0 = f(T)/V^*$ , and  $s_1 = k_B T/V^*$ . However, the observed temperature dependence of  $s_0$  and  $s_1$  does not follow simply from these relations. While  $s_0$  is approximately proportional to temperature [Fig. 1(b) inset],  $s_1$  varies slowly at high  $T$  and appears to approach a constant at low  $T$ . This would require  $V^* \rightarrow 0$  as  $T \rightarrow 0$ . It seems more likely that  $s_1$  is related to intrinsic rate effects. Several analytic models [5,6,10,11,20] include such effects, but their consequences have not been worked out for the entire rate-temperature-age parameter space.

It is interesting to compare the above data for the onset of yield to previous studies of the flow stress in steady-state shear [14,21]. Sheared systems cannot reach regime II in Fig. 3, because they are constantly being "rejuvenated" [3,19]. One expects that the effective waiting time should scale with the inverse shear rate, leading to logarithmic rate dependence with slope  $s_1 - s_0$  characteristic of regime I. The measured slope is indeed closer to that of regime I and is also relatively insensitive to temperature [14,21].

In conclusion, we have found a complex interplay of waiting time, temperature, and rate in determining the yield stress of glassy solids. In the absence of an imposed strain, the system evolves only through thermal activation. Aging leads to a logarithmic increase in density with a prefactor that decreases rapidly as  $T$  decreases. The state of the system continues to evolve through thermal activation during shear. The yield stress reflects both this evolution and intrinsic rate dependence. A unified description [Eq. (2)] based on rate-state models of friction [23,24] is able to collapse all data at each temperature onto a universal curve (Fig. 3). At large values of  $\dot{\epsilon}t_w$  (regime II), there is little evolution of the system as it is strained to yield and

$\tau^y$  rises rapidly with strain rate. At small values of  $\dot{\epsilon}t_w$  (regime I), the stress rises less rapidly with  $\dot{\epsilon}$  because the increase in stress with rate is partially offset by a reduction in the time for aging. The model can be obtained from a simple modification of the Eyring model, and the results may help test and motivate future analytic theories of plasticity in glassy materials. Experimental data [16] are qualitatively consistent with the model and should follow the universal collapse predicted by Eq. (2).

This research was supported in part by the National Science Foundation under Grants No. DMR-0454947 and No. PHY99-07949.

- 
- [1] R.N. Haward and R.J. Young, *The Physics of Glassy Polymers* (Chapman and Hall, London, 1997).
  - [2] J. Lu, G. Ravichandran, and W.L. Johnson, *Acta Mater.* **51**, 3429 (2003).
  - [3] A.J. Liu and S.R. Nagel, *Jamming and Rheology* (Taylor & Francis, London, 2001).
  - [4] M.L. Falk and J.S. Langer, *Phys. Rev. E* **57**, 7192 (1998).
  - [5] A. Lemaitre, *Phys. Rev. Lett.* **89**, 195503 (2002).
  - [6] M.L. Falk, J.S. Langer, and L. Pechenik, *Phys. Rev. E* **70**, 011507 (2004).
  - [7] D.J. Lacks, *Phys. Rev. Lett.* **87**, 225502 (2001).
  - [8] C. Maloney and A. Lemaitre, *Phys. Rev. Lett.* **93**, 016001 (2004).
  - [9] G. Picard, A. Ajdari, F. Lequeux, and L. Bocquet, *Phys. Rev. E* **71**, 010501(R) (2005).
  - [10] M. Fuchs and M.E. Cates, *Phys. Rev. Lett.* **89**, 248304 (2002).
  - [11] V. Kobelev and K.S. Schweizer, *Phys. Rev. E* **71**, 021401 (2005).
  - [12] K. Miyazaki, D.R. Reichman, and R. Yamamoto, *Phys. Rev. E* **70**, 011501 (2004).
  - [13] J. Rottler and M.O. Robbins, *Phys. Rev. E* **64**, 051801 (2001).
  - [14] J. Rottler and M.O. Robbins, *Phys. Rev. E* **68**, 011507 (2003); *Comput. Phys. Commun.* **169**, 177 (2005);
  - [15] L. Berthier, J.-L. Barrat, and J. Kurchan, *Phys. Rev. E* **61**, 5464 (2000); L. Berthier and J.-L. Barrat, *Phys. Rev. Lett.* **89**, 095702 (2002).
  - [16] L.C.E. Struik, *Physical Aging in Amorphous Polymers and Other Materials* (Elsevier, New York, 1978).
  - [17] C. Monthus and J.-P. Bouchaud, *J. Phys. A* **29**, 3847 (1996).
  - [18] W. Kob and J.-L. Barrat, *Phys. Rev. Lett.* **78**, 4581 (1997).
  - [19] M. Utz, P.G. Debenedetti, and F.H. Stillinger, *Phys. Rev. Lett.* **84**, 1471 (2000).
  - [20] S.M. Fielding, P. Sollich, and M.E. Cates, *J. Rheol. (N.Y.)* **44**, 323 (2000).
  - [21] F. Varnik, L. Bocquet, and J.-L. Barrat, *J. Chem. Phys.* **120**, 2788 (2004).
  - [22] W. Kob and H.C. Andersen, *Phys. Rev. E* **51**, 4626 (1995).
  - [23] J.H. Dieterich, *J. Geophys. Res.* **84**, 2169 (1979).
  - [24] A. Ruina, *J. Geophys. Res.* **88**, 10 359 (1983).
  - [25] D.J. Lacks and M.J. Osborne, *Phys. Rev. Lett.* **93**, 255501 (2004).
  - [26] H. Eyring, *J. Chem. Phys.* **4**, 283 (1936).